**ORIGINAL ARTICLE**

# SIRT6 Protects Against Myocardial Ischemia–Reperfusion Injury by Attenuating Aging-Related CHMP2B Accumulation

Xiaokang Li[1] · Lin Liu[2] · Wenhua Jiang[3] · Manling Liu[4] · Yishi Wang[4] · Heng Ma[4] · Nan Mu[4] · Haiyan Wang[1]

## Abstract

Impaired autophagic flux induces aging-related ischemia vulnerability, which is the hallmark pathology in cardiac aging. Our previous work has confirmed that the accumulation of charged multivesicular body protein 2B (CHMP2B), a subunit of the ESCRT-III complex, in the heart can impair autophagy flux. However, whether CHMP2B accumulation contributes to aging-related intolerance to ischemia/reperfusion (I/R) injury and the regulatory mechanism for CHMP2B in aged heart remain elusive. The cardiac CHMP2B level was significantly higher in aged human myocardium than that in young myocardium. Increased CHMP2B were shown to inhibit autophagic flux leading to the deterioration of MI/R injury in aged mice hearts. Interestingly, a negative correlation was observed between SIRT6 and CHMP2B expression in human heart samples. Specific activation of SIRT6 suppressed CHMP2B accumulation and ameliorated autophagy flux in aged hearts. Using myocardial-specific SIRT6 heterozygous knockout mice and recovery experiments confirmed that SIRT6 regulated myocardial CHMP2B levels. Finally, activation of SIRT6 decreased acetylation of FoxO1 to promote its transcriptional function on Atrogin-1, a muscle-specific ubiquitin ligase, which subsequently enhanced the degradation of CHMP2B by Atrogin-1. This is a novel mechanism for SIRT6 against aging-related myocardial ischemia vulnerability, particularly by preventing excessive accumulation of autophagy key factors.

Associate Editor Junjie Xiao oversaw the review of this article

Heng Ma, Nan Mu and Haiyan Wang contributed equally.

✉ Heng Ma
  hengma@fmmu.edu.cn

✉ Nan Mu
  muunan@fmmu.edu.cn

✉ Haiyan Wang
  wanghaiyan0329@vip.163.com

1  Department of Cardiology, Tangdu Hospital, Fourth Military Medical University, No. 1 Xinsi Rd, Xi'an, China

2  Department of Dermatology, Tangdu Hospital, Fourth Military Medical University, No. 1 Xinsi Rd, Xi'an 710032, China

3  Institute of Medical Research, Northwestern Polytechnical University, Xi'an, China

4  Department of Physiology and Pathophysiology, School of Basic Medicine, Fourth Military Medical University, No. 169 Changle West Rd, Xi'an, China

## Introduction

Ischemic heart disease is one of the leading causes of mortality and disability worldwide [1]. Aging is a risk factor associated not only with a progressive degeneration in physical function of heart, but also with a significant increase in stress-related damage. Aging hearts are vulnerable to cardiac diseases, and intrinsic aging-related physical deterioration makes the heart more susceptible to ischemia–reperfusion (I/R) injury [2–6]. Identifying the molecular basis of aging-related ischemic vulnerability is not only scientifically important, but also necessary for the discovery of new therapeutic targets.

Charged multivesicular body protein 2B (CHMP2B) is a component of the heteromeric endosomal sorting complex required for transport III (ESCRT-III) complex, which mediates the biogenesis of multivesicular bodies. Previous studies found that CHMP2B was highly expressed in neurons in all major regions of the brain, and that mutations in *CHMP2B* gene resulted in one form of familial frontotemporal lobar degeneration [7]. The knockdown and

mutation of CHMP2B could cause the abnormal aggregation of autophagosome-related membranes and proteins, which played important roles in neurodegenerative disease like Alzheimer's disease [8]. It was reported that CHMP2B not only participates in the disorder of autophagy flux in neural cells, but also plays important roles in cardiovascular diseases [9]. Failure of CHMP2B degradation in the heart results in autophagy impairment, intracellular protein aggregate accumulation, unfolded protein response activation, and subsequent cardiomyocytes apoptosis. In a previous study, we found that cardiomyocytes with I/R injury had upregulated CHMP2B expression, which led to impaired autophagic flux and deterioration of I/R injury [10]. Furthermore, the degradation of CHMP2B is regulated by Atrogin-1 (the protein encoded by gene *Fbxo32*), a muscle-specific ubiquitin-ligase that was originally identified as a mediator of muscle atrophy [9]. However, the function of CHMP2B in aged hearts and the exact molecular mechanisms of Atrogin-1-mediated CHMP2B degradation remain unclear.

Silent information regulator 6 (SIRT6), a member of the sirtuin family, is a nicotinamide adenine dinucleotide (NAD+)-dependent deacetylase with multiple roles in controlling cellular biology functions including antioxidant stress, senescence, metabolism, telomere maintenance, DNA repair, inflammation, and autophagy [5, 11]. Overexpression or activation of SIRT6 has been associated with improved myocardial function. Therefore, it acts as a protector against cardiovascular diseases such as cardiac hypertrophy, I/R injury, and heart failure [12–15]. In myocardial I/R injury, SIRT6 was demonstrated to counteract oxidative stress damage by activating FoxO3α in an adenosine-5'-monophosphate (AMP)-activated protein kinase (AMPK)-dependent manner, thus enhancing transcription of FoxO-dependent antioxidant genes [16]. Furthermore, the impairment of autophagy flux plays important roles in I/R-induced organ injury [17]. In the liver, SIRT6 has been shown to regulate autophagy throughout the process of I/R injury [18]. However, it is still unknown whether and how SIRT6 regulates autophagy in MI/R injury. FoxO transcription factors are the downstream targets regulated by SIRT6 and have key roles in aging-related I/R injury [19–21], implying that FoxO transcription factors may contribute greatly to the SIRT6-associated autophagy flux of aged hearts.

Here, we report that decreased SIRT6 expression causes CHMP2B accumulation in aging-related MI/R injury. Moreover, specific activation of SIRT6 reversed the impaired autophagy flux caused by CHMP2B accumulation through FoxO1-Atrogin-1 pathway, indicating a novel mechanism that SIRT6 is a potential therapeutic target in aging-related CHMP2B accumulation and myocardial ischemia vulnerability.

## Methods

### Animals and Human Samples

Male C57BL/6 mice (young: 3–4 months and aged: 22–24 months) were purchased from the animal center of the Fourth Military Medical University.

The inducible cardiac-specific-SIRT6-knockout (SIRT6 icKO) male mice were obtained from Prof. Liu BH from Shenzhen University. SIRT6 icKO were generated as previously reported [22]. Four-week-old mice that were positive for the Myh6-Cre ± transgene and had loxP sites flanking the SIRT6 gene (Shenzhen Key Laboratory for Systemic Aging and Intervention) were injected intraperitoneally with Tamoxifen (Solarbiol, Beijing, China; 75 mg/kg, i.p.) for seven consecutive days. Fifty milligrams of tamoxifen were dissolved in 1 ml of ethanol. Approximately 4.0 ml of corn oil (Solarbiol, Beijing, China) was added to get a final concentration of 10 mg/ml.

Both C57BL/6 mice and SIRT6 icKO mice were raised using the same method as previously described [3]. The mice were randomly assigned to each of the experimental groups. All animal experiments in this study were approved by the Animal Ethical Experimentation Committee of the Fourth Military Medical University.

Normal human myocardial tissues were obtained from paraffin-embedded tissue at the Pathology Department of Xijing Hospital, Fourth Military Medical University. All patients signed informed consent forms. The research protocol was designed and executed according to the principles of the Declaration of Helsinki and was approved by the ethics review board of Fourth Military Medical University. The median age of the 15 samples was 46 (range: 35–68 years), and 40% of the samples were female (Supplementary Table). Subjects with cardiomyopathy or disease with potential myocardial changes (high blood pressure, stroke, heart failure, hyperglycemia, dementia, abnormal hepatic and renal function, and acute diseases) were excluded from this study.

### Antibodies and Reagents

Rabbit anti-CHMP2B (76,173), rabbit anti-p62 (5114), rabbit anti-LC3B (3868), rabbit anti-FoxO1 (2880), rabbit anti-H3(4499), and rabbit anti-Atg5 (12,994) antibodies were purchased from Cell Signaling Technology (Danvers, MA, USA). Rabbit anti-Atrogin-1 (Muscle atrophy box F gene 1, ab168372), rabbit anti-SIRT6 (ab191385), and rabbit anti-LAMP1 (ab24170) antibodies were procured from Abcam (Cambridge, MA, USA). Mouse anti-H3K9ac

(PTM-156), mouse anti-H3K18ac (PTM-158), and mouse anti-H3K56ac (PTM-162) were purchased from PTM BIO (Hangzhou, China). Rabbit anti-CHMP2B (12,527–1-AP) for immunohistochemistry was procured from Proteintech (Wuhan, China), whereas rabbit anti-SIRT6 (PA5-95,240) for immunohistochemistry was obtained from Invitrogen (Carlsbad, CA, USA).

The proteasome inhibitor MG-132 (HY-13259) and the FoxO1 inhibitor AS1842856 (HY-100596) were purchased from MedChem Express (MCE, Princeton, NJ, USA). Professor Jian Zhang of Shanghai Jiao-Tong University School of Medicine provided MDL800, which is an allosteric activator of SIRT6 [23].

## The Treatment of Inhibitor/Promoters

In vivo: MDL800 was dissolved in DMSO (20,688, Thermo, Waltham, MA, USA) and injected into mice via tail vein at a dosage of 150 mg/kg/day for 3 days before the MI/R surgery. Mice were injected intraperitoneally with 10 mg/kg/day of AS1842856, which was also dissolved in DMSO, for 7 days prior to MDL800 treatment.

In vitro: H9c2 cells were co-incubated with MDL800 (50 μM) for 48 h prior to H/R injury (Supplementary Fig. 1). During the last 8 h of co-incubation, a concentration of 10 μM reagent was added into the medium with MDL800 for MG132 treatment.

## Small Interference RNA and Adenovirus Virus Transfection

A 20 μM small interference RNA (siRNA) stock solution was prepared by dissolving 1 OD unit of siRNA in 250 μL of $H_2O$. The stock solution was stored in small aliquots at − 20 °C. H9c2 cells were grown on coverslips in six-well plates, and when the cells reached about 30~40% confluency, a lipofectamine 2000 reagent (Invitrogen, Carlsbad, CA, USA) was used to transfect si-Atrogin-1 (100 nM, Tsingke Biotechnology Co., Ltd., Beijing, China), scramble siRNA (si-NC), and si-FoxO1 (100 nM, Ribobio, Guangzhou, China) into cells following the manufacturer's instructions [24]. The target sequences of si-FoxO1 and si-Atrogin-1 were 5′-GCA AGTTTATTCGAGTACA-3′ and 5′-ACUUUAAGCUUG UGCGAUG-3′, respectively [25].

Adenovirus-expressing CHMP2B (Ad-CHMP2B) was purchased from GemmaPharma (Shanghai, China). H9c2 cells were grown on coverslips in six-well plates at about 30~40% confluency. Ad-CHMP2B was added to the cell media at a titer of $1.0 \times 10^{10}$ PFU/ml and transfected for 24 h before any additional treatment.

## HBAD-mcherry-EGFP-LC3 Assay

HBAD-mcherry-EGFP-LC3 virus, an adenovirus tool for researching autophagy flux was procured from HanBiol ($2.5 \times 10^{10}$ PFU/ml; Shanghai, China). Cells were transfected with HBAD-mcherry-EGFP-LC3 virus 24 h after Ad-CHMP2B transfection using the same methods as Ad-CHMP2B transfection. After 24 h of transfection, the cells with autophagy express LC3 protein with both red (mcherry) and green (EGFP) fluorescence, and the formation of autophagolysosomes leads to the loss of green fluorescence without any effect to red fluorescence. Cells were subjected to H/R injury and then fixed in 4% paraformaldehyde by incubation for 15 min at room temperature, followed by nuclei staining with DAPI (Duolink®) using in situ mounting medium. The counts of different color spots reflects the strength of the autophagic flux, with more yellow fluorescence indicating that the autophagosome and lysosome fusion is inhibited and the autophagolysosome process is blocked.

## Adeno-Associated Virus Infection

Recombinant adeno-associated virus (AAV; serotype 9) vectors expressing mouse SIRT6 with a c-TNT promoter (AAV9-SIRT6; Hanbio Inc., Shanghai, China) was used to overexpress SIRT6 in vivo. AAV9-EGFP was used as a negative control. As previously reported [26], SIRT6 icKO mice were injected with 100 μL virus at a concentration of $1.2 \times 10^{12}$ vg/ml in the tail vein one week after injection with tamoxifen (mice at 6 weeks). Myocardial SIRT6 expression was analyzed 4 weeks after the injection of virus.

## Ischemia and Reperfusion Surgery In Vivo

MI/R mouse in vivo model was established as previously described [3]. Young and aged male C57BL/6 mice were subjected to MI/R surgery at the day after the last tail vein injection with MDL800. And the MI/R surgery was conducted 4 weeks after the injection of virus in SIRT6 icKO mice (mice at 10 weeks). Both C57BL/6 mice and SIRT6 icKO mice were subjected to the same MI/R surgical method. Briefly, mice were anesthetized with 2% isoflurane, intubated, and ventilated using a rodent ventilator (Taimeng Co. Ltd., Chengdu, China). The chest was opened at the fourth intercostal space, and the anterior surface of the heart was exposed to locate the proximal left anterior descending artery (LAD), which was then wrapped with a 6–0 silk Ethilon suture and tightened to achieve cardiac ischemia. Sham-operated animals were used as surgical controls and underwent sham-operation excluding ligation of the LAD. After occlusion for 30 min, reperfusion was performed by loosening the ligature.

## Cell Culture and In Vitro Hypoxia/Reoxygenation Treatment

H9c2 cells (Procell Life Science & Technology Co. Ltd., Wuhan, China) were cultured in Dulbecco's modified Eagle's medium (PM150210, Procell Life Science & Technology Co. Ltd., Wuhan, China) supplemented with 10% certified fetal bovine serum (VivaCell, Shanghai, China) and 1% penicillin/streptomycin (Solarbiol, Beijing, China).

For in vitro hypoxia/reoxygenation (H/R) treatment, the H9c2 cells were incubated in Dulbecco's modified Eagle's medium (DMEM) glucose-free with L-glutamine (G4527, Servicebio, Wuhan, China) in Modular Incubator Chamber (Billups-Rothenberg, Inc., Del Mar, CA, USA) with a gas mixture (95% $N_2$ and 5% $CO_2$) for 8 h at 37 ℃ and then reoxygenated for 12 h (95% air and 5% $CO_2$) [27].

## Western Blotting and Co-Immunoprecipitation

The heart tissues were obtained immediately after the surgery of MI/R. Similarly, cultured cells were obtained immediately after the treatment of H/R. Western blotting was performed as previously described [19]. Briefly, tissues and cells were lysed in a lysis buffer (tissue protein extraction reagent or mammalian protein extraction reagent, Thermo, Waltham, MA, USA) containing protease and phosphatase inhibitor mini tablets (A32959, Thermo, Waltham, MA, USA). After adequate lysis and centrifugation at 12,000 $g$ for 10 min at 4 °C, cell supernatant was extracted, and protein concentration was measured using a BCA protein assay kit (Thermo, Waltham, MA, USA). Protein was mixed with $5 \times$ SDS-PAGE loading buffer (CW0027, CoWin Biosciences, Jiangsu, China) and heated at 95 °C for 10 min. Denatured samples were separated on a 10% SDS–polyacrylamide gel before being transferred to PVDF membranes. The membranes were blocked with 5% non-fat milk for 1 h at room temperature, and then incubated with primary antibodies overnight at 4 °C, followed by incubation with horseradish peroxidase-conjugated secondary antibodies for 1 h at room temperature. After addition of chemiluminescent fluid (WBKLS0500, Millipore, MA, USA) to the membrane, the proteins were visualized, and the results were analyzed using ImageJ, which is bundled with 64-bit Java 1.8.0_172 (National Institutes of Health).

The direct interaction between Atrogin-1 and CHMP2B in cells was examined using co-immunoprecipitation [10]. Cell lysates were incubated with an anti-CHMP2B or anti-Atrogin-1 antibody, together with Dynabeads Protein G (Invitrogen, Carlsbad, CA, USA) according to the manufacturer's protocol and identified using western blot methods as previously described [19]. VeriBlot for IP Detection Reagents (ab131366) were used to detect the co-immunoprecipitated protein without masking by the IgG heavy (50 kDa) and light (25 kDa) chains.

## Immunohistochemistry and Quantification of IHC Staining

Immunohistochemistry was performed as previously described [3]. All immunostained sections were observed and photographed using an automatic digital slide scanner (Pannoramic MIDI II).

Immunostaining intensity was quantified using the ImageJ program, which is bundled with 64-bit Java 1.8.0_172 (National Institutes of Health).

## Quantitative Real-Time PCR

The real-time PCR was performed as previously described [16]. TRIzol reagent (15,596,018, Invitrogen, Carlsbad, CA, USA) was used to extract total RNA, which was then reverse transcribed into cDNA. For real-time assays, PCR reactions were prepared in TB Green Premix Ex Taq (Takara Bio, Dalian, China). The following primer sequences were used in this study: FoxO1: forward 5′-GGCGGGCTGGAAGAA TTCAA-3′ and reverse 5′-ACTCTTGCCTCCCTCTGG AT-3′; Atrogin-1: forward 5′-GGGAGTACTAAGGAG CGCCA-3′ and reverse 5′-CCACTCAGGGATGTGAGC TG-3′; GAPDH: forward 5′-ACAGCAACAGGGTGGTGG AC-3′ and reverse 5′-TTTGAGGGTGCAGCGAACTT-3′. The mRNA levels of FoxO1 and Atrogin-1 were normalized to GAPDH. Above primers were synthesized by Tsingke Biotechnology Co., Ltd (Beijing, China).

## Cell Viability Assay

Cell viability was quantified using the Cell Counting Kit-8 (Mishushengwu, Xian, China) as previously described [28]. Briefly, 100 μl of H9c2 cell medium were replaced with fresh culture medium. 10 μl of CCK-8 solution were then added into each well. A microplate reader (Molecular Devices, CA, USA) was used to measure absorbance at 450 nm after 1 h of incubation at 37 ℃.

## Lactate Dehydrogenase Assay

Blood samples from mice were collected 24 h after reperfusion and centrifuged to obtain serum. Furthermore, the culture medium was collected 2 h after reoxygenation and centrifuged to obtain supernatant. The concentrations of LDH were analyzed using spectrophotometry as previously described [3].

## TUNEL Fluorescent Assay

TUNEL fluorescent assay was conducted using freshly frozen sections of LV and the Fluorescein (FITC) Tunel Cell Apoptosis Detection Kit (Servicebio, Wuhan, China) following the manufacturer's protocols [29]. The sections were counter-stained with DAPI (1:1000) for 5 min, washed three times with PBS, and covered with a microscopic glass for further study. The TUNEL-positive cells were counted and analyzed by an investigator who was blinded to the treatment conditions.

## Echocardiography Procedure

Transthoracic echocardiography was performed 1 week after the MI/R surgery. Resting mice were anaesthetized with 2.0% isoflurane. All hair was removed from the chest with a chemical hair remover. Examination was performed using a high-resolution imaging system for small animals (a Vevo 3100 imaging system, Visual Sonics). The ejection fraction (LVEF) and fractional shortening (LVFS) were determined from parasternal short axis M-mode images.

## Chromatin Immunoprecipitation Analysis

Chromatin immunoprecipitation (ChIP) was performed using the EZ-Magna ChIP™ A/G Chromatin Immunoprecipitation Kit (Sigma, MA, USA) following the manufacturer's instructions [30]. Briefly, H9c2 cells were transfected with pCMV-FoxO1 or si-FoxO1 and cross-linked with 1% formaldehyde. Chromatin fragmentation was performed through enzymatic digestion according to the kit instructions. A diluted soluble chromatin solution was incubated with a ChIP grade rabbit anti-FoxO1 antibody for 18 h at 4 ℃ with rotation. A non-immune rabbit IgG was used as a negative control. The bound products were washed after incubation with protein A/G beads, and DNA was eluted. A Chromo4 Real-Time PCR Detection System (Bio-Rad Life Sciences) was used to amplify specific Atrogin-1 promoter sequences using DNA as a template. Primers (forward 5′-CAAGGTTGTGCAACTGCGAG-3′, reverse 5′-GAT AGGACGGATCGACAGCC-3′), which targeted a 395 bp fragment of the rat Atrogin-1 promoter were used for PCR amplification.

## Vector Construction and Dual Luciferase Reporter Assays

The WT-Fbxo32 luciferase reporter vector (the gene of Atrogin-1, Gene ID:171,043) was constructed by synthesizing the sequence 2100 bp upstream of the *Fbxo32* transcription start site, whereas the mutant-Fbxo32 (binding sites mutant) vector was constructed using a Q5 Site-Directed Mutagenesis Kit (E0554S, New England Biolabs, Beijing, China).

H9c2 cells were seeded in a 24-well plate. The cells were cultured overnight before being transfected with luciferase reporter plasmids (Control vectors, WT-Fbxo32 containing FoxO1 binding sites, and mutant-Fbxo32 containing mutant sequences of FoxO1 binding sites). Luciferase assays were performed using the dual luciferase reporter assay system (Promega, WI, USA) 48 h after transfection.

## Statistical Analysis

All data were presented as mean ± standard error of the mean. To determine statistical differences between groups, a one-way analysis of variance was performed, followed by a Dunnett's test post-hoc test. All statistical analyses were performed using GraphPad Prism 8.0 (GraphPad Software, San Diego, CA, USA). Statistical significance was considered when $p \leq 0.05$.

# Results

## Cardiac CHMP2B Accumulation and Autophagic Defects with Aging

CHMP2B immunohistochemical (IHC) score was performed in human myocardial samples. We found a significant correlation between age and CHMP2B expression in human heart, indicating that CHMP2B accumulated in aged hearts (Fig. 1A). This phenomenon was also found in mouse hearts, which had considerably higher levels of CHMP2B protein expression in aged heart than young hearts, as shown by immunohistochemistry staining and western blot (Fig. 1B, C). Furthermore, western blot revealed a significantly increased level of Atg5, LC3II, p62 and LAMP1 (Fig. 1C), indicating impaired autophagy flux in aged cardiomyocytes, which was in line with our previous study [3].

To identify the condition of CHMP2B expression and autophagy flux in aging-related MI/R injury, we used a MI/R injury model in young and aged male C57BL/6 mice, with the left anterior descending artery clamped for 30 min followed by reperfusion for 4 h. MI/R injury induced an increased expression level of CHMP2B in hearts from young mice (Fig. 1D), which was consistent with our previous study [10]. Moreover, we found an additional increase in CHMP2B accumulation and autophagy flux impairment in aged hearts with I/R injury (Fig. 1D). These results indicated that the accumulation of CHMP2B, as well as the resulting impairment of autophagy flux, was involved in the pathological process of I/R injury in aged hearts.
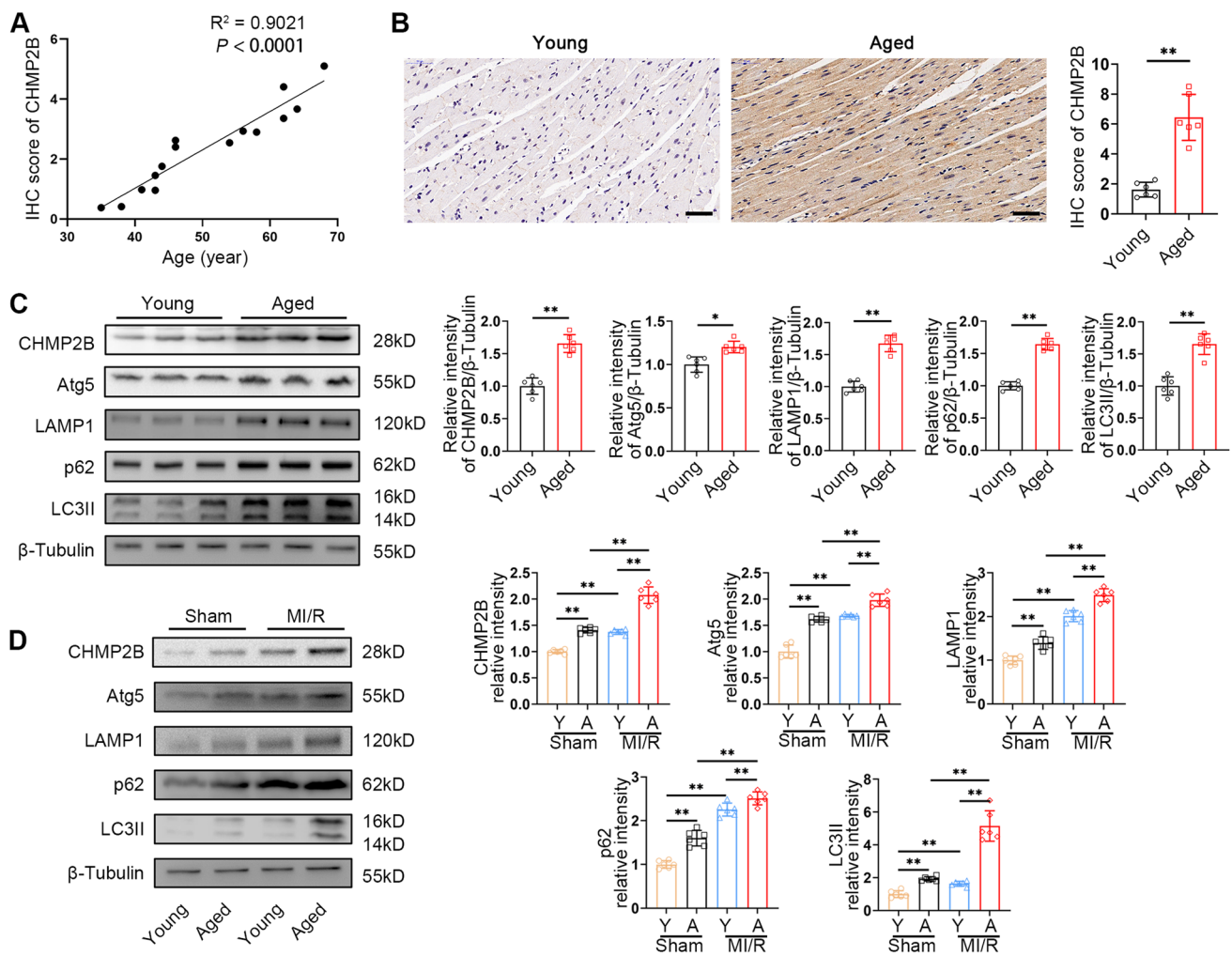
**Fig. 1** CHMP2B accumulation impaired autophagy flux in aging-related MI/R injury. **A** Correlation between immunohistochemical (IHC) scores of CHMP2B and ages of normal human heart samples ($n = 15$). **B** Representative immunohistochemistry staining images of CHMP2B expressions in heart tissues from young and aged mice (bar = 50 μm) and quantitative analysis of CHMP2B staining scores (right, $n = 6$). **C** Protein expression levels of CHMP2B and its down-stream molecules that are involved in autophagy in heart tissues from young and aged mice were evaluated by Western blot. Densitometry analysis on protein levels of CHMP2B, Atg5, LAMP1, p62, and LC3II ($n = 6$). **D** After MI/R surgery, young and aged hearts were analyzed by Western blot for protein expression levels of CHMP2B, Atg5, LAMP1, p62, and LC3II ($n = 6$, Y: young, A: aged). Data are presented as mean ± SD. *$P < 0.05$; **$P < 0.01$

## SIRT6 Negatively Regulated Myocardial CHMP2B Protein Level

SIRT6 has been reported to play an essential role in aging and ischemia–reperfusion injury prevention [31, 32]. Newly, we observed a significantly negative correlation between SIRT6 and CHMP2B expression in human heart samples (Fig. 2A). We also observed a decrease in SIRT6 expression in aged hearts and a further decrease after MI/R injury, whereas CHMP2B exhibited the opposite trend of expression as SIRT6 (Fig. 2B). These results indicated that SIRT6 may negatively regulate CHMP2B.

To identify the role of SIRT6 in regulating CHMP2B expression, we examined the changes in CHMP2B expression levels after activating SIRT6 using its specific promoter MDL800. The activation of SIRT6 was confirmed by a reduction in acetylated histone H3K9, H3K18, and H3K56 after MDL800 treatment in aged mice with MI/R injury (Fig. 2C). The activation of SIRT6 markedly decreased CHMP2B protein level in MI/R hearts and modified the associated autophagy disorder, evidenced by the reduction of Atg5, LC3 II/I, p62, and LAMP1 levels (Fig. 2C). Furthermore, MDL800 treatment protected the heart from MI/R-induced injury, as demonstrated by decreased levels of
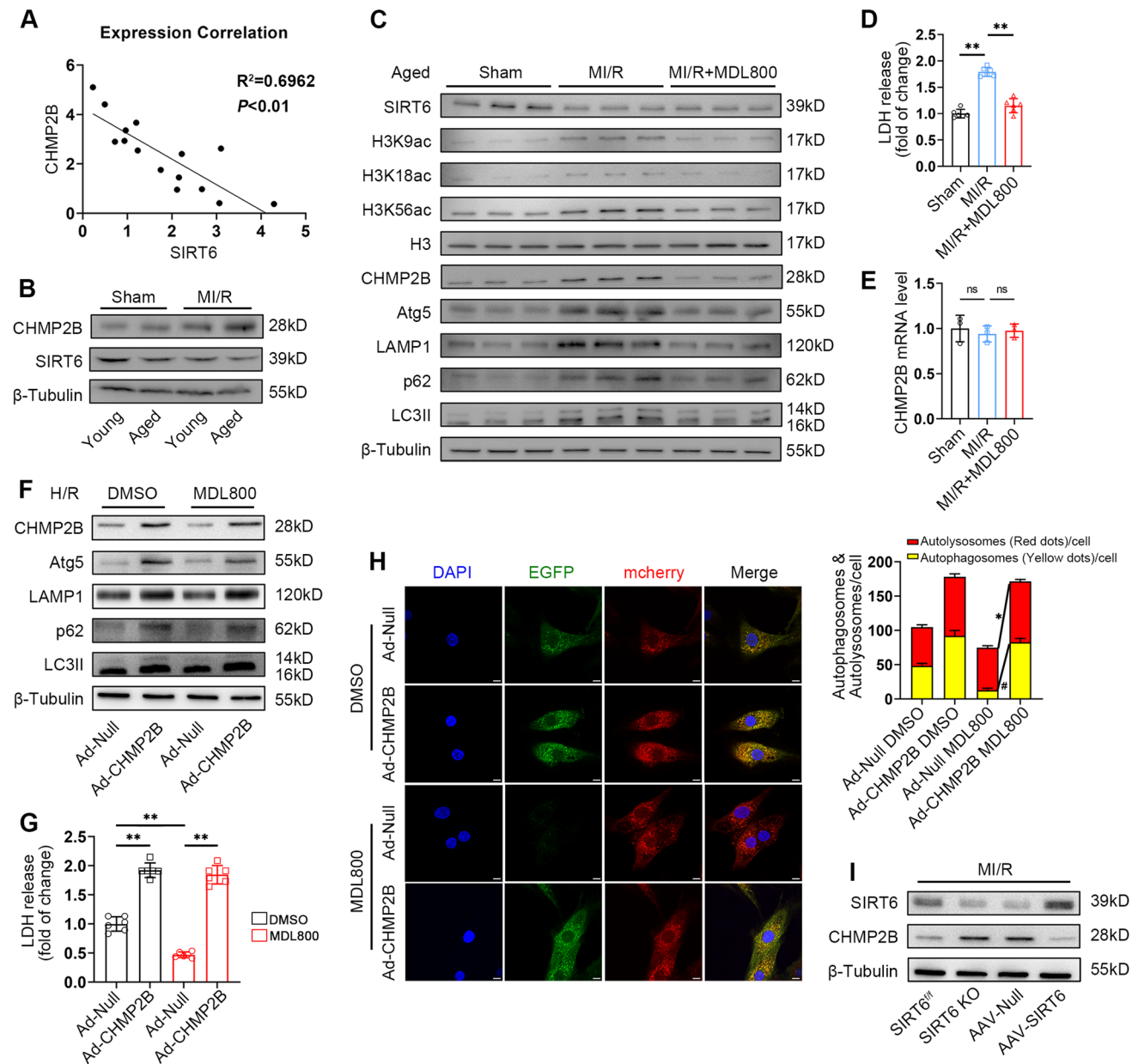
**Fig. 2** SIRT6 regulates protein expression levels of CHMP2B in aging-related MI/R injuries. **A** Correlations between SIRT6 and CHMP2B expression levels in normal human heart samples ($n=15$). **B** Protein expression levels of CHMP2B and SIRT6 in heart tissues from young and aged mice with or without MI/R surgery were analyzed by Western blot ($n=6$). **C** Expression levels of SIRT6, total H3 and acetylated H3, CHMP2B, Atg5, LAMP1, p62 as well as LC3II in heart tissues of aged mice treated with DMSO or MDL800 before MI/R surgery were evaluated by Western blot ($n=6$). **D** Serum LDH levels were evaluated in MI/R injured mice after treatment with DMSO or MDL800 ($n=6$). **E** mRNA expression levels of CHMP2B in mice heart tissues were evaluated by RT-PCR ($n=3$). **F** H9c2 cells were transfected with Ad-CHMP2B and treated with DMSO or MDL800 before H/R injury. Expression levels of CHMP2B and associated autophagy molecules were evaluated by Western blot ($n=6$).

**G** LDH levels in supernatants were evaluated after H/R injury cells had been transfected with Ad-CHMP2B and treated with DMSO or MDL800 ($n=6$). **H.** Representative images of fluorescent LC3 puncta after HBAD-mcherry-EGFP-LC3 adenovirus transduction (24 h) and analysis of the autophagosome (yellow) and autophagolysosome (red) in control cells or Ad-CHMP2B group with or without MDL800 treatment before H/R injury ($n=3$, bar $=10$ μm). **I.** Mice with heart specific SIRT6 transgene containing flox (SIRT6$^{flox/flox}$) were treated with tamoxifen to induce SIRT6 knockout (SIRT6 icKO) phenotypes and some mice were further transfected with adeno-associated virus to overexpress SIRT6 (AAV-SIRT6). These three groups of mice were subjected to MI/R surgery after which SIRT6 and CHMP2B levels were evaluated by Western blot ($n=6$). Data are presented as mean $\pm$ SD. *$P<0.05$; **$P<0.01$; #$P<0.01$; n.s., non-significant

LDH (Fig. 2D). However, MDL800 treatment had no effect on CHMP2B mRNA expression (Fig. 2E), indicating that SIRT6 mainly regulated myocardial CHMP2B protein level.

To confirm the effect of CHMP2B on cardioprotection of SIRT6 against I/R injury, we overexpressed CHMP2B in H9c2 cells before MDL800 treatment under the condition of H/R injury. The results showed that MDL800 treatment reduced the expression of CHMP2B and autophagy molecules (Fig. 2F) and the LDH levels in H/R-treated H9c2 cells (Fig. 2G), which was consistent with the findings in vivo. However, overexpression of CHMP2B blocked the protective effect of MDL800 on H/R-treated H9c2 cells evidenced by increased re-elevated LDH levels (Fig. 2G) without any effect on the expression level of SIRT6 (Supplementary Fig. 2). We also conducted the HBAD-mcherry-EGFP-LC3 assay to analyze the dynamic changes of autophagy flux. When the cells show yellow fluorescence, it indicates that the autophagosome clearance is impaired. In vitro fluorescence results showed that MDL800 treatment lowered the level of yellow fluorescence, indicating improved of autophagosome clearance, whereas overexpression of CHMP2B resulted in crippled autophagosome clearance (Fig. 2H). These results revealed that CHMP2B was necessary for the regulation of SIRT6 activation on autophagy and protection against MI/R injury.

To validate these results, we conducted MI/R surgery on mice with myocardial specific SIRT6 heterozygous knocked-out (SIRT6 icKO). The expression of SIRT6 was significantly decreased by about 50% in the hearts of SIRT6 icKO mice compared to the control group (SIRT6$^{flox/flox}$). Furthermore, the deficiency of endogenous SIRT6 caused a significant increase in CHMP2B levels in MI/R hearts (Fig. 2I). On the contrary, we used AAV-SIRT6 adeno-associated virus to restore the expression of myocardial SIRT6 in SIRT6 icKO mice. The injection of AVV-SIRT6 upregulated the expression of SIRT6 while significantly decreased the level of CHMP2B in cardiomyocytes in SIRT6 icKO mice (Fig. 2I). These results revealed that SIRT6 has an inhibitory regulation on the expression of CHMP2B in aged hearts with MI/R injury.

## SIRT6 Promoted Atrogin-1 Mediated CHMP2B Degradation

Our and other previous research found that Atrogin-1 regulates the degradation of CHMP2B [9, 10, 33]. To explore the mechanism by which SIRT6 regulates CHMP2B protein levels, we observed the effect of specific activation of SIRT6 on Atrogin-1 in the H/R model of H9c2 cells. MDL800 treatment (50 μM for 24 h) on H9c2 cells promoted Atrogin-1 expression, lowered CHMP2B levels (Fig. 3A), and protected H9c2 cells against H/R injury as demonstrated by increased cell viability (Fig. 3B) and suppression of LDH

concentration (Fig. 3C). Moreover, the proteasome inhibitor MG132 blocked the inhibitory effect of SIRT6 on CHMP2B expression, with significantly higher levels of CHMP2B in the MDL800 and MG132 treatment groups (Fig. 3A). It also suppressed cell viability and increased LDH levels (Fig. 3B and C), indicating that the MG132 attenuated the myocardial protection role of MDL800.

To test the interaction of Atrogin-1 and CHMP2B, we conducted the CO-IP assay on H9c2 cells under MDL800 treatment or H/R injury. The results revealed that MDL800 treatment improved the correlation of CHMP2B and Atrogin-1 in the presence or absence of H/R (Fig. 3D). Furthermore, we transfected siRNA targeting Atrogin-1 into H9c2 cells and found that the interference of Atrogin-1 blocked the suppression of MDL800 on CHMP2B expression (Fig. 3E). These results demonstrated that the inhibitory effect of SIRT6 on CHMP2B was achieved by Atrogin-1.

## FoxO1 Mediated the Transcriptional Regulation of Atrogin-1 by SIRT6

SIRT6 was found to activate the FoxO pathway in cardiomyocytes [16]. We next hypothesized that SIRT6 may regulate the expression of Atrogin-1 via the FoxO pathway.

As predicted in JASPAR database, FoxO1 is an Atrogin-1 transcription factor with several potential binding targets on the promoter of *Fbox32* (Atrogin-1 gene) (Fig. 4A). According to the locations and sequences of predicted binding targets, we designed specific primers for CHIP assays in H9c2 cells. The CHIP assays results showed amplified DNA bands in the group of chromatins immunoprecipitated with FoxO1 antibody, and the intensity of DNA bands increased in the FoxO1 overexpressed group (pCMV-FoxO1) and decreased in the FoxO1 interfered group (si-FoxO1; Fig. 4B), confirming that FoxO1 transcriptionally promoted the expression of Atrogin-1 in cardiomyocytes. The luciferase reporter system results confirmed the direct binding of FoxO1 to *Fbox32* promoter. Moreover, mutations in the region of the predicted binding sites significantly inhibited the effect of FoxO1 on *Fbox32* promoter activation (Fig. 4C). These results demonstrated that FoxO1 transcriptionally regulates Atrogin-1.

To test the effect of FoxO1 regulation, we transfected FoxO1 siRNA into H9c2 cells and detected a decrease in Atrogin-1 and an increase in CHMP2B levels (Fig. 4D). In line with the aforementioned results, MDL800 treatment of H9c2 cells with H/R injury increased Atrogin-1 expression, suppressed CHMP2B accumulation (Fig. 4E), and protected against H/R injury by increasing cell viability (Fig. 4F) and decreasing LDH concentration (Fig. 4G). However, the interference of FoxO1 expression by specific siRNA inhibited the
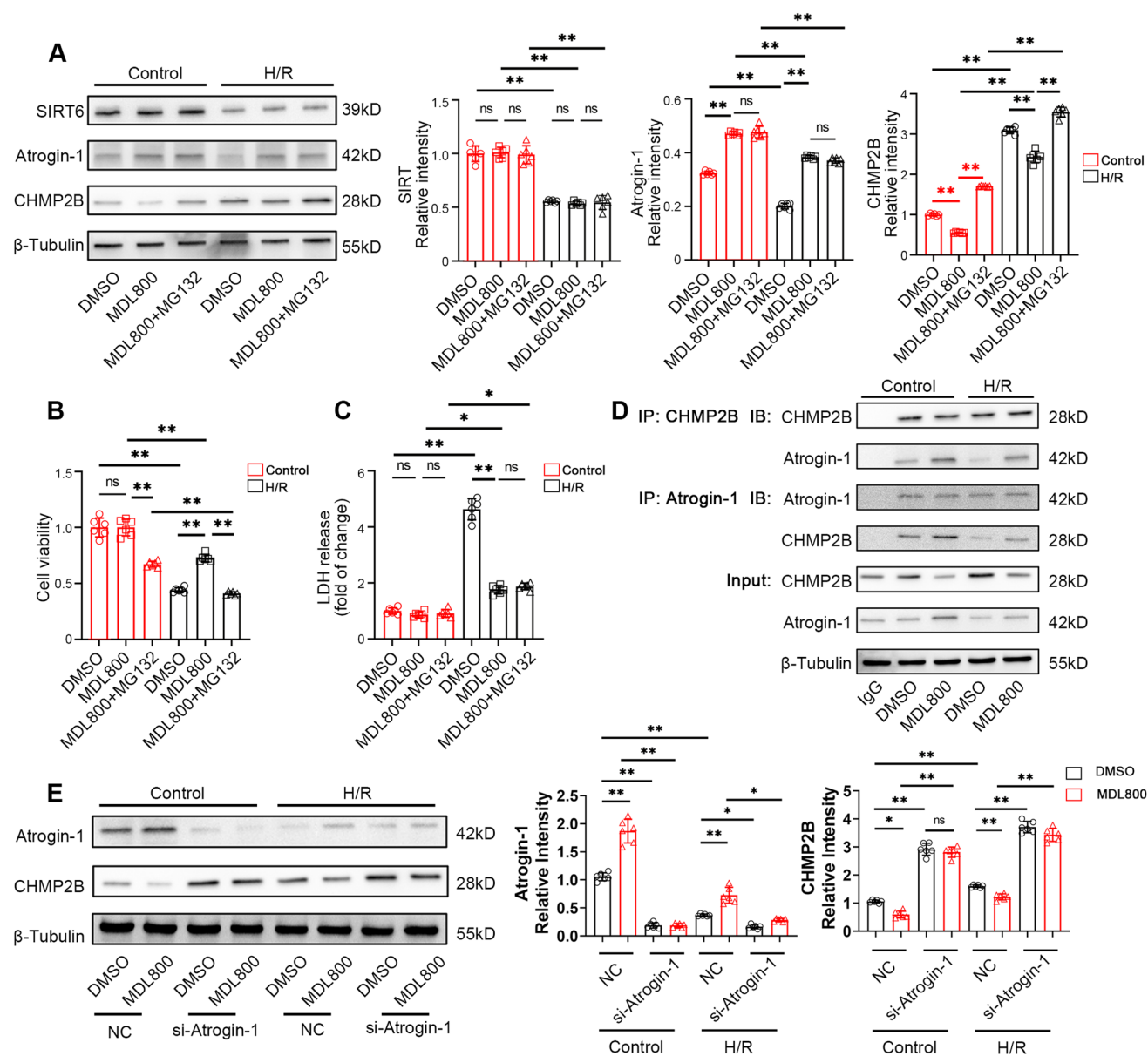
**Fig. 3** SIRT6 promotes Atrogin-1 mediated degradation of CHMP2B in cardiomyocytes with H/R. **A** H9c2 cells were treated with H/R and DMSO, MDL800 (50 μM for 24 h) or MG132 (10 μM for 8 h). Expression levels of SIRT6, Atrogin-1 and CHMP2B were assessed by Western blot ($n=6$). **B.** Viabilities of H9c2 cells with or without H/R were evaluated after DMSO, MDL800 (50 μM for 48 h) or MG132 (10 μM for 8 h) treatment ($n=6$). **C.** LDH levels in H9c2 cells with or without H/R were evaluated after treatment with DMSO,

MDL800 (50 μM for 48 h) or MG132 (10 μM for 8 h) ($n=6$). **D** Immunoprecipitation was performed to evaluate the relationship between Atrogin-1 and CHMP2B. H9c2 cells treated with MDL800 were subjected to immunoblotting analysis. **E** si-Atrogin-1(100 nM) was transfected into H9c2 cells with or without H/R, after which they were treated with MDL800 (50 μM), then, Atrogin-1 and CHMP2B levels were evaluated by Western blot (n=6). Data are presented as mean ± SD. *$P < 0.05$; **$P < 0.01$; n.s., non-significant

promotion of MDL800 treatment on Atrogin-1 expression (Fig. 4E) and blocked the myocardial protective role of SIRT6 simulation as demonstrated by the H/R injury assay (Fig. 4F and G). These findings indicated that the promotion of SIRT6 on Atrogin-1 expression was mediated by FoxO1.

## SIRT6 Activation Attenuates the MI/R Injury in Aged Hearts *via the* FoxO1-Atrogin-1-CHMP2B Pathway

The above results have shown that the activation of SIRT6 decrease the expression of CHMP2B in aged heart with I/R injury and the regulation of SIRT6 on CHMP2B was through
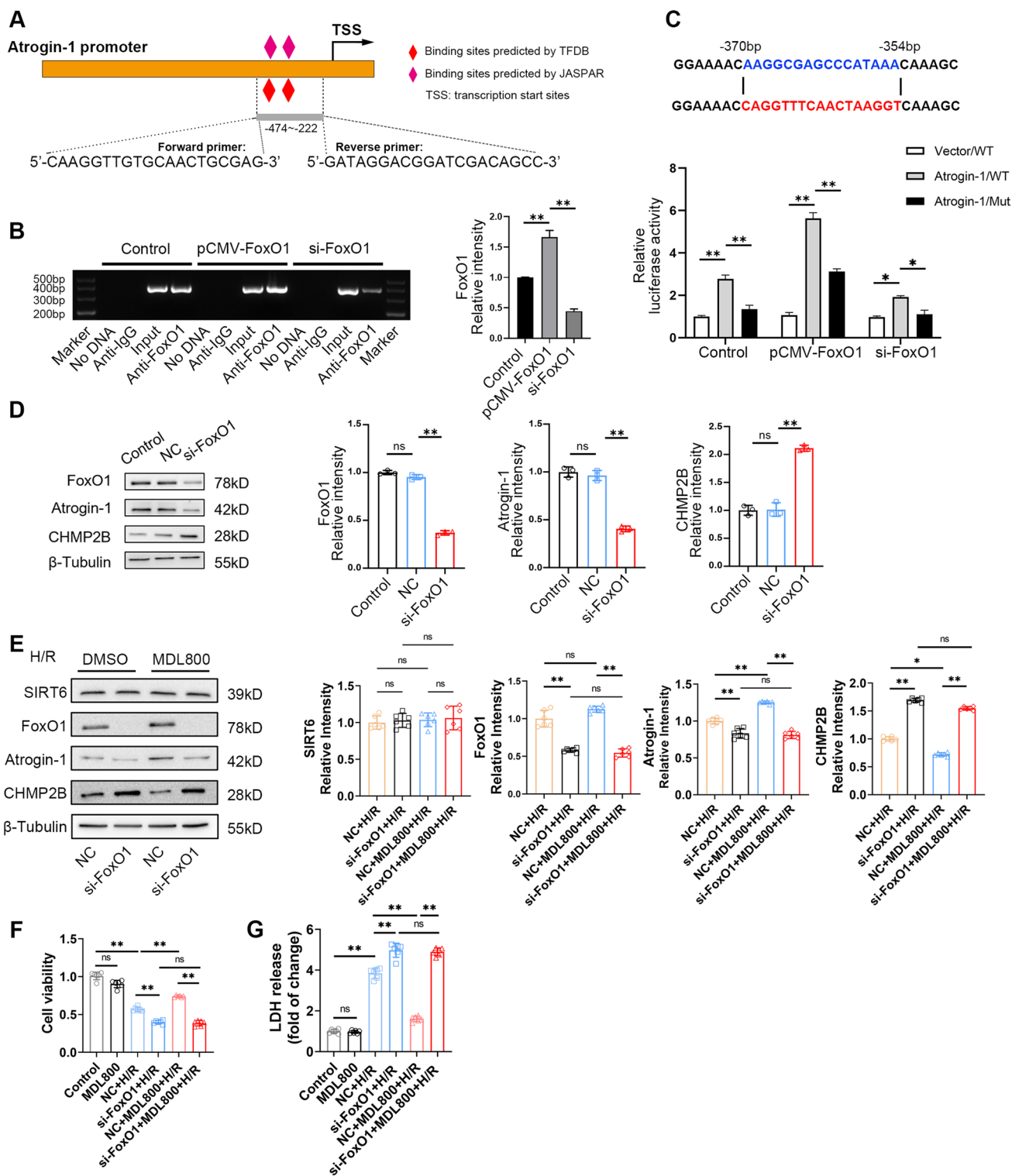
FoxO1-Atrogin-1 pathway. In young and aged mice hearts, the injury of I/R also decrease the expression of FoxO1 and Atrogin-1(Supplementary Fig. 3), which provides further evidence for our results of mechanism studies.

To verify the mechanisms discovered in vitro, we tested the regulation of SIRT6 on the FoxO1-Atrogin-1 pathway

in aged mice with MI/R injury. MDL800 treatment substantially enhanced Atrogin-1 expression while decreasing CHMP2B accumulation in aged hearts with I/R injury (Fig. 5A and Supplementary Fig. 4). Furthermore, we used AS1842856 on aged mice with MI/R injury after MDL800 to block the activation of FoxO1 when SIRT6 was stimulated

◄**Fig. 4** SIRT6 decreased CHMP2B levels in cardiomyocytes with H/R via the FoxO1-Atrogin-1 axis. **A** Binding targets predicted by JASPAR and TFDB website were marked on the Atrogin-1 promoter model. Primers used for the ChIP assay were also marked at predicted sites. **B** Chromatin immunoprecipitation (ChIP) assays (left) and quantification of ChIP results (right) to confirm direct binding of FoxO1 to Atrogin-1 promoter in H9c2 cells, which were left untreated (Control) or transfected with pCMV-FoxO1 (5 μg) or si-FoxO1(100 nM). **C** Relative luciferase activities of luciferase reporter plasmids containing the wild-type Atrogin-1 promoter (Atrogin-1/WT) or its mutant (Atrogin-1/Mut) in H9c2 cells transfected with the plasmids overexpressing FoxO1 (pCMV-FoxO1) or siRNA targeting FoxO1 (si-FoxO1) ($n = 3$). Above sequences show the FoxO1 binding motif (blue) and its mutant (red). **D** Protein levels of FoxO1, Atrogin-1 and CHMP2B in cells transfected with si-FoxO1 were evaluated by Western blot ($n = 3$). **E** Representative Western blot images showing the expression levels of SIRT6, FoxO1, Atrogin-1, and CHMP2B in H/R H9c2 cells after si-FoxO1 transfections with or without MDL800 (50 μM for 24 h). Densitometry of western blotting results was also analyzed ($n = 6$). **F and G** Quantification data for cell viability (F) and LDH concentrations (G) were calculated for control cells or cells subjected to H/R with or without MDL800 (50 μM for 24 h) or si-FoxO1 treatment ($n = 6$). Data are presented as mean ± SD. $*P < 0.05$; $**P < 0.01$; n.s., non-significant

[34]. The results demonstrated that AS1842856 treatment substantially reduced the expression of Atrogin-1 and increased CHMP2B level compared to the MDL800 group (Fig. 5A). In MI/R injury assays, cardiac contractile function improved considerably after MDL800 treatment but decreased with AS1842856 treatment (Fig. 5B). This result was supported by TTC staining (Fig. 5C), LDH secretion level in blood (Fig. 5D), and TUNEL staining (Fig. 5E), indicating that the activation of FoxO1was necessary in the regulation of SIRT6 on CHMP2B expression and the protection against MI/R injury.

Collectively, these results indicated that the FoxO1 pathway was required for the promotion of SIRT6 on Atrogin-1 mediated CHMP2B degradation in aged hearts with I/R injury and that stimulating SIRT6 improved autophagy flux and cardiac function via the FoxO1-Atrogin-1 pathway.

## Discussion

In this study, we demonstrated that CHMP2B accumulation impaired myocardial autophagic flux resulting in MI/R injury enhancement in aged hearts. Newly, through in vivo and in vitro experiments, SIRT6 activation was shown to decrease myocardial CHMP2B levels and, therefore, prevented aging-related myocardial ischemic vulnerability. Here, we demonstrate that, in the heart, Atrogin-1 mediated protein degradation effectively prevented CHMP2B accumulation. Mechanistic investigation found that SIRT6 upregulated Atrogin-1 transcription through FoxO1 in MI/R

myocardium, improving autophagic flux and reducing myocardial ischemic injury in aged mice.

Ischemic heart disease and myocardial infarction are essential causes of mortality in both young and elderly populations [35]. Activated autophagy has a positive effect on myocardial ischemia, while functional autophagy is vital in reducing oxidative stress, restoring energy substrates, and eliminating damaged mitochondria, all of which can induce myocardial cell death [17, 36]. Autophagy can be activated during stress to minimize damage and preserve cardiac functioning during MI/R, to inhibit ischemic-associated heart remodeling, and to induce changes in myocardial protein homeostasis. The misfolded protein accumulation is one pattern of cardiac adaptation to pressure overload. Previously, we reported the relationship between autophagic impairment and MI/R injury [3, 10, 37, 38]. Aging may cause impaired protein quality control, dysfunctional protein accumulation, and proteostasis imbalance, all of which increase vulnerability to MI/R injury [39]. In aged hearts, over-accumulation of autophagic components can lead to inhibition of myocardial autophagy and worsen MI/R injury.

CHMP2B is a key player in autophagy process and it is an important subunit of ESCRT-III, which is a complex responsible for many cellular processes including autophagy. In nervous system, the knockdown or mutation of CHMP2B impair the formation of ESCRT-III complex and cause abnormal aggregation of autophagosome-related membranes and proteins. However, the accumulation of CHMP2B also impairs autophagy flux [7]. Our group has found that CHMP2B accumulation impairs cardiac autophagy and enhances the vulnerability of the cardiac system to I/R injury [10]. Furthermore, we proved that CHMP2B is the substrate degraded by Atrogin-1, and that Atrogin-1 degrades CHMP2B via the ubiquitin-dependent pathway [10]. However, the function of CHMP2B in aged hearts, as well as the exact molecular mechanisms of Atrogin-1-mediated CHMP2B degradation, remains unknown.

SIRT6 is a NAD + -dependent deacetylase that is implicated in the regulation of lifespan, genomic stability, telomere integrity, transcription, and DNA repair [5, 11]. A recent study has shown that SIRT6 can mitigate aging-related cardiomyocyte senescence and cardiac hypertrophy [13]. In addition, inhibiting cell aging via SIRT6/AMPK autophagy may ameliorate diabetic myocardial fibrosis [40]. However, whether and how SIRT6 regulates functional autophagy in aged hearts is yet to be fully elucidated. Recently, a novel type of selective activator of SIRT6 was described [23]. MDL800 is a novel potent and selective allosteric activator of SIRT6. We found that MDL800 greatly decreased the impact of I/R injury on the aged hearts in mice via the SIRT6-mediated Atrogin-1-CHMP2B signalling axis.
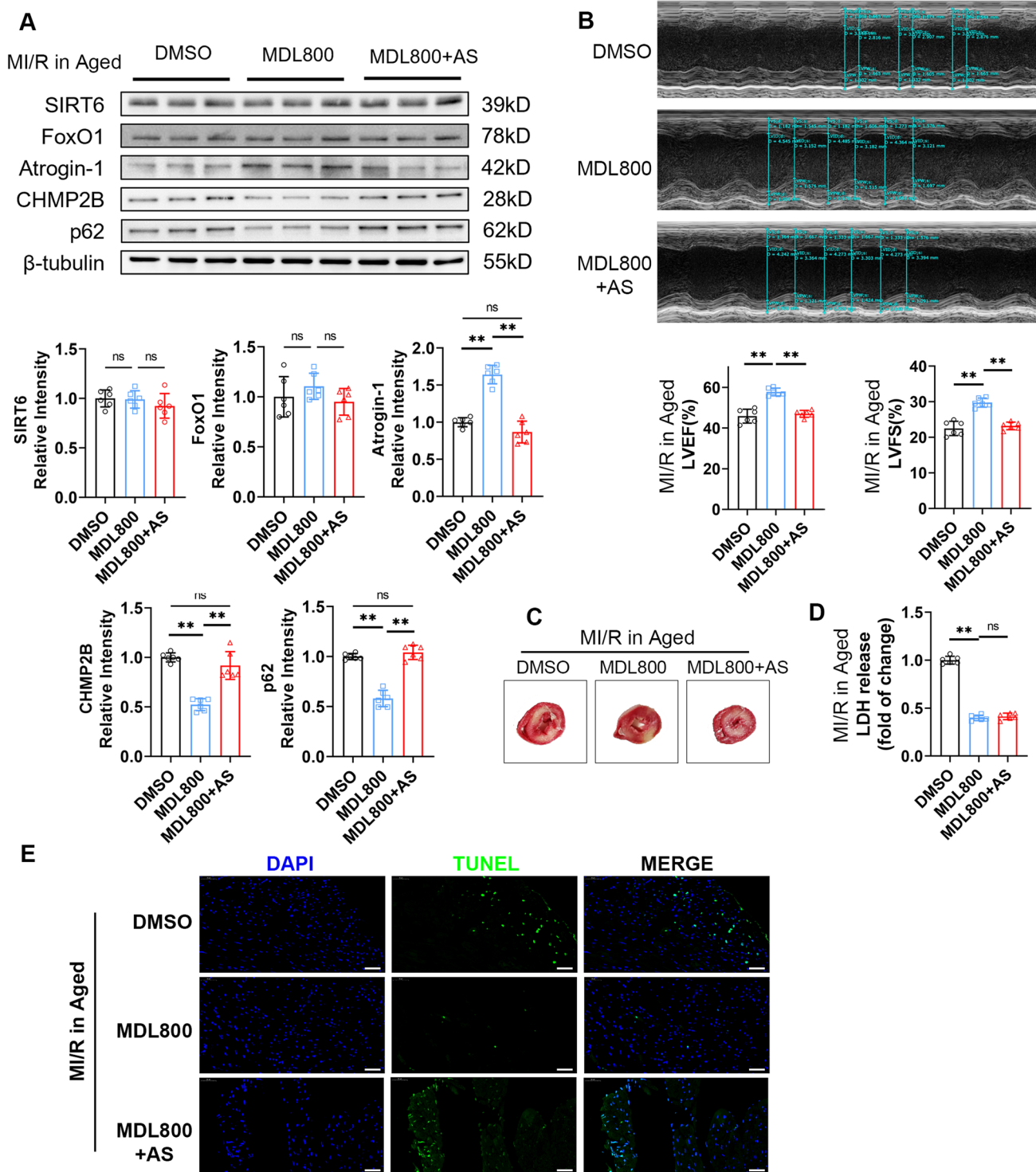
**Fig. 5** Activation of SIRT6 attenuated MI/R injury in aged mice through the FoxO1-Atrogin-1-CHMP2B pathway. **A** Aged mice were treated with MI/R and DMSO, MDL800 (150 mg/kg) or AS1842856 (10 mg/kg) as indicated. SIRT6, FoxO1, Atrogin-1, CHMP2B, and p62 levels were evaluated by Western blot (*n*=6). **B** Representative photomicrographs and average data for left ventricle ejection fraction (LVEF) and fractional shortening (LVFS) in mice were assessed by echocardiography after treatment as shown in panel A (*n*=6). **C** Representative samples of areas of infarct in hearts subjected to I/R injury (*n*=6). **D** Serum LDH levels were in MDL800 or MDL800 and AS treated mice subjected to MI/R injury (*n*=6). **E** TUNEL staining for hearts with MI/R injury treated with MDL800 or MDL800 and AS (*n*=6, bar=50 μm). Data are presented as mean±SD. *$P<0.05$; **$P<0.01$; n.s., non-significant

In summary, findings from this study, in clinical samples and animal experiments, provided new evidence that CHMP2B accumulates in aged myocardium, which lead to autophagy dysfunction and ischemic vulnerability. This study also found the mechanism link between SIRT6 and CHMP2B. Specific activation of SIRT6 increased the transcription level of Atrogin-1 through FoxO1 to enhance the degradation of CHMP2B. This is a novel mechanism that enriches the understanding of the mechanisms involved in SIRT6 mediated anti-aging ability and cardioprotection against MI/R injury, especially the regulation of key autophagic factors.

## Declarations

**Ethics Approval** All the procedures in this study were in accordance with the Helsinki Declaration of 1975, as revised in 2000, and were approved by the ethical review board of Fourth Military Medical University (IACUC-20200602). Informed consents were obtained from all study participants. Institutional and national guidelines for the care and use of laboratory animals were followed and approved by the appropriate institutional committees.

**Conflict of Interest** The authors declare no competing interests.

## References

1. GBD 2017 Causes of Death Collaborators. (2018). Global, regional, and national age-sex-specific mortality for 282 causes of death in 195 countries and territories, 1980–2017: a systematic analysis for the Global Burden of Disease Study 2017. *Lancet, 392*(10159), 1736–1788.

2. Ma, H., Wang, J., Thomas, D. P., Tong, C., Leng, L., Wang, W., et al. (2010). Impaired macrophage migration inhibitory factor-AMP-activated protein kinase activation and ischemic recovery in the senescent heart. *Circulation, 122*(3), 282–292.

3. Li, C., Mu, N., Gu, C., Liu, M., Yang, Z., Yin, Y., et al. (2020). Metformin mediates cardioprotection against aging-induced ischemic necroptosis. *Aging Cell, 19*(2), e13096.

4. Ren, J., & Zhang, Y. (2018). Targeting autophagy in aging and aging-related cardiovascular diseases. *Trends in Pharmacological Sciences, 39*(12), 1064–1076.

5. Li, X., Liu, L., Li, T., Liu, M., Wang, Y., Ma, H., et al. (2021). SIRT6 in senescence and aging-related cardiovascular diseases. *Frontiers in Cell and Developmental Biology, 9*, 641315.

6. Pietri, P., & Stefanadis, C. (2021). Cardiovascular Aging and Longevity: JACC State-of-the-Art Review. *Journal of the American College of Cardiology, 77*(2), 189–204.

7. Krasniak, C. S., & Ahmad, S. T. (2016). The role of CHMP2BIntron5 in autophagy and frontotemporal dementia. *Brain Research, 1649*(Pt B), 151–157.

8. Feng, Q., Luo, Y., Zhang, X. N., Yang, X. F., Hong, X. Y., Sun, D. S., et al. (2020). MAPT/Tau accumulation represses autophagy flux by disrupting IST1-regulated ESCRT-III complex formation: A vicious cycle in Alzheimer neurodegeneration. *Autophagy, 16*(4), 641–658.

9. Zaglia, T., Milan, G., Ruhs, A., Franzoso, M., Bertaggia, E., Pianca, N., et al. (2014). Atrogin-1 deficiency promotes cardiomyopathy and premature death via impaired autophagy. *Journal of Clinical Investigation, 124*(6), 2410–2424.

10. Li, T., Yin, Y., Mu, N., Wang, Y., Liu, M., Chen, M., et al. (2021). Metformin-enhanced cardiac AMP-activated protein kinase/Atrogin-1 pathways inhibit charged multivesicular body protein 2b accumulation in ischemia–reperfusion injury. *Frontiers in Cell and Developmental Biology, 8*, 621509.

11. Korotkov, A., Seluanov, A., & Gorbunova, V. (2021). Sirtuin 6: Linking longevity with genome and epigenome stability. *Trends in Cell Biology, S0962–8924*(21), 00125–00132.

12. Khan, D., Ara, T., Ravi, V., Rajagopal, R., Tandon, H., Parvathy, J., et al. (2021). SIRT6 transcriptionally regulates fatty acid transport by suppressing PPARγ. *Cell Reports, 35*(9), 109190.

13. Pillai, V. B., Samant, S., Hund, S., Gupta, M., & Gupta, M. P. (2021). The nuclear sirtuin SIRT6 protects the heart from developing aging-associated myocyte senescence and cardiac hypertrophy. *Aging (Albany NY), 13*(9), 12334–12358.

14. Grootaert, M., Finigan, A., Figg, N. L., Uryga, A. K., & Bennett, M. R. (2021). SIRT6 protects smooth muscle cells from senescence and reduces atherosclerosis. *Circulation Research, 128*(4), 474–491.

15. Yu, L. M., Dong, X., Xue, X. D., Xu, S., Zhang, X., Xu, Y. L., et al. (2021). Melatonin attenuates diabetic cardiomyopathy and reduces myocardial vulnerability to ischemia-reperfusion injury by improving mitochondrial quality control: Role of SIRT6. *Journal of Pineal Research, 70*(1), e12698.

16. Wang, X., Wang, X., Tong, M., Gan, L., Chen, H., Wu, S., et al. (2016). SIRT6 protects cardiomyocytes against ischemia/reperfusion injury by augmenting FoxO3α-dependent antioxidant defense mechanisms. *Basic Research in Cardiology, 111*(2), 13.

17. Aghaei, M., Motallebnezhad, M., Ghorghanlu, S., Jabbari, A., Enayati, A., Rajaei, M., et al. (2019). Targeting autophagy in cardiac ischemia/reperfusion injury: A novel therapeutic strategy. *Journal of Cellular Physiology, 234*(10), 16768–16778.

18. Zhang, S., Jiang, S., Wang, H., Di, W., Deng, C., Jin, Z., et al. (2018). SIRT6 protects against hepatic ischemia/reperfusion injury by inhibiting apoptosis and autophagy related cell death. *Free Radical Biology & Medicine, 115*, 18–30.

19. Shi, M. Y., Bang, I. H., Han, C. Y., Lee, D. H., Park, B. H., & Bae, E. J. (2020). Statin suppresses sirtuin 6 through miR-495, increasing FoxO1-dependent hepatic gluconeogenesis. *Theranostics, 10*(25), 11416–11427.

20. Spurthi, K. M., Sarikhani, M., Mishra, S., Desingu, P. A., Yadav, S., Rao, S., et al. (2018). Toll-like receptor 2 deficiency hyperactivates the FoxO1 transcription factor and induces aging-associated cardiac dysfunction in mice. *Journal of Biological Chemistry, 293*(34), 13073–13089.

21. Hsu, C. P., Zhai, P., Yamamoto, T., Maejima, Y., Matsushima, S., Hariharan, N., et al. (2010). Silent information regulator 1 protects

the heart from ischemia/reperfusion. *Circulation, 122*(21), 2170–2182.

22. Peng, L., Qian, M., Liu, Z., Tang, X., Sun, J., Jiang, Y., et al. (2020). Deacetylase-independent function of SIRT6 couples GATA4 transcription factor and epigenetic activation against cardiomyocyte apoptosis. *Nucleic Acids Research, 48*(9), 4992–5005.

23. Huang, Z., Zhao, J., Deng, W., Chen, Y., Shang, J., Song, K., et al. (2018). Identification of a cellularly active SIRT6 allosteric activator. *Nature Chemical Biology, 14*(12), 1118–1126.

24. Yang, Y., Duan, W., Lin, Y., Yi, W., Liang, Z., Yan, J., et al. (2013). SIRT1 activation by curcumin pretreatment attenuates mitochondrial oxidative damage induced by myocardial ischemia reperfusion injury. *Free radical biology & medicine, 65*, 667–679.

25. Castillero, E., Alamdari, N., Lecker, S. H., & Hasselgren, P. O. (2013). Suppression of atrogin-1 and MuRF1 prevents dexamethasone-induced atrophy of cultured myotubes. *Metabolism-Clinical and Experimental, 62*(10), 1495–1502.

26. Li, C., Sun, W., Gu, C., Yang, Z., Quan, N., Yang, J., et al. (2018). Targeting ALDH2 for Therapeutic Interventions in Chronic Pain-Related Myocardial Ischemic Susceptibility. *Theranostics, 8*(4), 1027–1041.

27. Zafir, A., Readnower, R., Long, B. W., McCracken, J., Aird, A., Alvarez, A., et al. (2013). Protein O-GlcNAcylation is a novel cytoprotective signal in cardiac stem cells. *Stem Cells, 31*(4), 765–775.

28. Zheng, J., Zhao, S., Yu, X., Huang, S., & Liu, H. Y. (2017). Simultaneous targeting of CD44 and EpCAM with a bispecific aptamer effectively inhibits intraperitoneal ovarian cancer growth. *Theranostics, 7*(5), 1373–1388.

29. Xu H, Yu W, Sun S, Li C, Ren J, Zhang Y. (2021). TAX1BP1 protects against myocardial infarction-associated cardiac anomalies through inhibition of inflammasomes in a RNF34/MAVS/NLRP3-dependent manner. *Science Bulletin, 66*(16), 1669–1683.

30. Li, Z., Zhang, H., Chen, Y., Fan, L., & Fang, J. (2012). Forkhead transcription factor FOXO3a protein activates nuclear factor kappaB through B-cell lymphoma/leukemia 10 (BCL10) protein and promotes tumor cell survival in serum deprivation. *Journal of Biological Chemistry, 287*(21), 17737–17745.

31. Mostoslavsky, R., Chua, K. F., Lombard, D. B., Pang, W. W., Fischer, M. R., Gellon, L., et al. (2006). Genomic instability and aging-like phenotype in the absence of mammalian SIRT6. *Cell, 124*(2), 315–329.

32. Kanfi, Y., Naiman, S., Amir, G., Peshti, V., Zinman, G., Nahum, L., et al. (2012). The sirtuin SIRT6 regulates lifespan in male mice. *Nature, 483*(7388), 218–221.

33. Sandri, M., Sandri, C., Gilbert, A., Skurk, C., Calabria, E., Picard, A., et al. (2004). Foxo transcription factors induce the atrophy-related ubiquitin ligase atrogin-1 and cause skeletal muscle atrophy. *Cell, 117*(3), 399–412.

34. Wang, D., Wang, Y., Zou, X., Shi, Y., Liu, Q., Huyan, T., et al. (2020). FOXO1 inhibition prevents renal ischemia-reperfusion injury via cAMP-response element binding protein/PPAR-gamma coactivator-1alpha-mediated mitochondrial biogenesis. *British Journal of Pharmacology, 177*(2), 432–448.

35. Virani, S. S., Alonso, A., Benjamin, E. J., Bittencourt, M. S., Callaway, C. W., Carson, A. P., et al. (2020). Heart disease and stroke statistics-2020 update: A report from the American Heart Association. *Circulation, 141*(9), e139–e596.

36. Heusch, G. (2020). Myocardial ischaemia-reperfusion injury and cardioprotection in perspective. *Nature Reviews Cardiology, 17*(12), 773–789.

37. Ma, H., Guo, R., Yu, L., Zhang, Y., & Ren, J. (2011). Aldehyde dehydrogenase 2 (ALDH2) rescues myocardial ischaemia/reperfusion injury: Role of autophagy paradox and toxic aldehyde. *European Heart Journal, 32*(8), 1025–1038.

38. Wang, Y., Yang, Z., Zheng, G., Yu, L., Yin, Y., Mu, N., et al. (2019). Metformin promotes autophagy in ischemia/reperfusion myocardium via cytoplasmic AMPKα1 and nuclear AMPKα2 pathways. *Life Sciences, 225*, 64–71.

39. Sciarretta, S., Maejima, Y., Zablocki, D., & Sadoshima, J. (2018). The Role of autophagy in the heart. *Annual Review of Physiology, 80*, 1–26.

40. Li, Y., Liu, M., Song, X., Zheng, X., Yi, J., Liu, D., et al. (2020). Exogenous hydrogen sulfide ameliorates diabetic myocardial fibrosis by inhibiting cell aging through SIRT6/AMPK autophagy. *Frontiers in Pharmacology, 11*, 1150.

**Publisher's Note** Springer Nature remains neutral with regard to jurisdictional claims in published maps and institutional affiliations.